Chemical Engineering Science 306 (2025) 121292

Contents lists available at ScienceDirect

Chemical Engineering Science

journal homepage: www.elsevier.com/locate/ces

# Development of a novel thermochemical cycle without electrolysis step to produce hydrogen

Sibel Uygun Batgi *, Ibrahim Dincer

*Clean Energy Research Laboratory, FEAS-OTU, Oshawa, Ontario, Canada*

ARTICLE INFO

*Keywords:*
Thermochemical cycle
Hydrogen production
Cu-Cl Cycle
Efficiency
Environmental impact
Sustainable development

ABSTRACT

This study presents a new three-step copper-chlorine (Cu-Cl) cycle that can operate with heat input without electrolysis step. While the sensitivity analyses of the system are performed to evaluate the system performance through the Aspen Plus, thermodynamic analyses of the system are performed with energetic and exergetic approaches. The highest exergy destruction among the components in the system was the decomposition reactor with a rate of 50.6 %. Furthermore, the energy and exergy values for the simulated system to produce 1 mol of hydrogen are determined by calculating the energy requirements of all components in the system. The total energy required for the system to generate 1 mol of hydrogen is calculated to be 997.81 kJ/mol $H_2$. The system's decomposition reactor is identified as the component that necessitated the most energy, with a value of 504.76 kJ/mol $H_2$. Moreover, the overall energy and exergy efficiencies are calculated to be 72.50 % and 46.70 %, respectively.

## 1. Introduction

From past to present, energy consumption globally has been increasing as the world's population and industrialization increase. The main reasons for this increase include increasing wealth level, urbanization and rising energy-based living standards. Today, the required energy demand mostly comes from fossil-based energy sources (Attia, 2024). Since fossil fuels such as coal, natural gas, and oil (Razmjoo et al., 2021) are widely used in energy generation, they have many negative environmental impacts (Abdullaev et al., 2023). The combustion of fossil fuels emits greenhouse gases into the atmosphere, therefore giving rise to significant environmental negative impacts (Kazi et al., 2021) such as global warming and climate change, the limited availability of these resources also poses risks in terms of energy security (Márquez-Ramos, 2018). Therefore, turning to sustainable, environmentally friendly and renewable energy sources is important to meet the energy needs of the future and reduce environmental impacts (Montignac et al., 2024). Hydrogen is an essential alternative energy source (Drawer et al., 2024) that can decrease the need for fossil fuels (Ozsari, 2023). It is an environmentally benign energy source that does not includes carbon atoms in its structure (Southall and Khare, 2016) and releases solely water vapor after combustion. While the usage of hydrogen in several areas makes it suitable for industrial usage, it also makes it important for the long-term storage of renewable energies and it utilize as a clean fuel (Abanades et al., 2006). However, since it does not exist in free form in nature, special methods are used to produce hydrogen. Today, hydrogen generation is mostly based on technologies that use fossil-based fuels. Hydrogen obtained from fossil fuels is generally produced by steam methane reforming (SMR) (Dilmaç and Özkan, 2008), and this method causes the release of $CO_2$ (Powell and Edgar, 2012). If $CO_2$ is not captured, it will have a negative impact on the environment. Therefore, hydrogen must be produced with clean production methods integrated with renewable energy sources (Southall and Khare, 2016). The renewable energy-based hydrogen production methods can provide an environmentally friendly and sustainable option. In this context, many studies have been carried out, especially on the electrolysis method (Ajeeb et al., 2024). Electrolysis enables the production of green hydrogen when integrated with renewable energy sources, facilitating long-term energy storage (Mishra et al., 2024). However, electrolysis method provides a low efficiency value of 18–24 % in the overall process (Velasquez-Jaramillo et al., 2024).

In order to clearly understand the environmental impacts of different hydrogen production methods, many studies have been presented in the literature comparing the Global Warming Potential (GWP) and Eco-indicator values. One of these studies was presented by Li et al. (2024). The results obtained from this study are presented in Fig. 1. It compares the environmental impacts of different hydrogen production

* Corresponding author.
*E-mail addresses:* sibel.uygun@ontariotechu.ca (S.U. Batgi), Ibrahim.Dincer@ontariotechu.ca (I. Dincer).

https://doi.org/10.1016/j.ces.2025.121292
Received 30 October 2024; Received in revised form 5 January 2025; Accepted 27 January 2025
Available online 30 January 2025
0009-2509/© 2025 The Author(s). Published by Elsevier Ltd. This is an open access article under the CC BY-NC-ND license (http://creativecommons.org/licenses/by-nc-nd/4.0/).

**Nomenclature**

| | |
|---|---|
| Ce-Cl | Cerium-chloride |
| Cu-Cl | Copper-chlorine |
| Cu-$SO_4$ | Copper-sulfate |
| eq | equivalent |
| $\dot{E}x_D$ | Exergy destruction rate (kW) |
| $\dot{E}x^Q$ | Exergy rate of heat transfer (kW) |
| Fe-Cl | Iron-chlorine |
| $h$ | Specific enthalpy (kJ $kg^{-1}$) |
| $h_0$ | Specific enthalpy at reference conditions (kJ $kg^{-1}$) |
| $\dot{m}$ | Mass flow rate (kg $s^{-1}$) |
| $\dot{n}$ | Mol flow rate (mol $s^{-1}$) |
| $\dot{Q}$ | Thermal energy rate (kW) |
| $\dot{S}$ | Entropy rate (kJ $kg^{-1}$ $K^{-1}$ $s^{-1}$) |
| $T_0$ | Ambient temperature (°C and K) |
| $\dot{W}$ | Work rate (kW) |
| $\dot{W}_{pump}$ | Pump work rate (kW) |

*Greek letters*

| | |
|---|---|
| η | Energy efficiency |
| Ψ | Exergy efficiency |

*Subscripts*

| | |
|---|---|
| b | boundary |
| ch | chemical |
| dec | decomposition |
| dest | destruction |
| e | electricity |
| ex | exergy |
| en | energy |
| g | gas |
| gen | generation |
| hyd | hydrolysis |
| in | input |
| l | liquid |
| o | Reference state |
| Ph | physical |
| prod | production |
| s | solid |
| sep | separator |

*Acronyms*

| | |
|---|---|
| AEA | Aspen Energy Analyzer |
| DIPPR | Design Institute for Physical Properties |
| EBE | Energy Balance Equation |
| EES | Engineering Equation Solver |
| EnBE | Entropy Balance Equation |
| ExBE | Exergy Balance Eguation |
| GGE | Gasoline Gallon Equivalent |
| GWP | Global Warming Potential |
| HHV | Higher Heating Value |
| LHV | Lower Heating Value |
| MCFC | Molten Carbonate Fuel Cell |
| MBE | Mass Balance Equation |
| NIST | National Institute of Standards and Technology |
| SCWR | Super Critical Water-Cooled Reactor |
| SMR | Steam Methane Reforming |
| SMR | Small Modular Reactor |
| TWS | Thermochemical Water Splitting |
| UNIQAC | Universal Quasi-Chemical |

methods in terms of GWP and eco-indicator values. GWP expresses the contribution of greenhouse gases released into the atmosphere during the production of one kilogram of hydrogen to global warming in terms of carbon dioxide equivalent (g $CO_2$-eq/ kg $H_2$). Eco-indicator is an indicator that measures the overall environmental impacts of the production process and combines multiple factors such as resource consumption, human health and effects on the ecosystem and results in a unit value. According to Fig. 1, natural gas steam reforming has a high GWP value of approximately 12,000 g $CO_2$-eq/kg $H_2$ and an eco-indicator value of approximately 30,000 units. This shows that this method has a very high impact on global warming and general environmental impacts. In renewable and nuclear energy-based methods, environmental impacts are seen to be highly reduced. In particular, the nuclear-based Cu-Cl cycle stands out as one of the environmentally friendly hydrogen production methods with a value of approximately 700 g $CO_2$-eq/kg $H_2$. These data clearly show that renewable and nuclear-based hydrogen production methods are more advantageous in terms of environmental sustainability compared to fossil fuel-based methods. In particular, the nuclear-based Cu-Cl cycle stands out as a strong candidate in hydrogen production due to its ability to minimize environmental impacts.

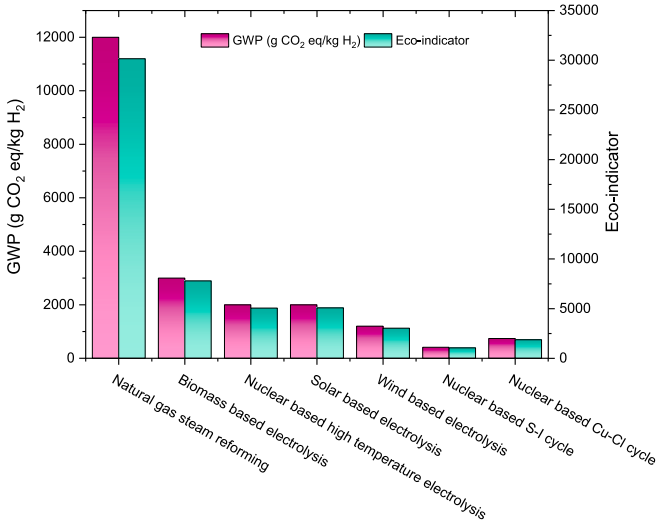



**Fig. 1.** The GWP and eco-indicator values of various hydrogen production methods (data from (Li et al., 2024)).

Since the 1970s, various thermochemical cycles have been developed as alternatives to water electrolysis. These thermochemical cycles could be more efficient than water electrolysis, thanks to the thermodynamic advantages of reactions at high temperatures, and require less electrical energy to produce the same amount of hydrogen (Bertino et al., 2024). As part of the U.S. Department of Energy's Nuclear Hydrogen Initiative, Argonne National Laboratory identified the most commercially promising thermochemical cycles as Cu-Cl, copper sulfate (Cu-$SO_4$), chlorine (Ce-Cl), vanadium-chlorine (V-Cl), cerium- magnesium iodine (Mg-I), iron-chlorine (Fe-Cl), hybrid chlorine, and active metal alloy cycles. During the evaluation process, parameters such as maximum working temperature, thermodynamic efficiency, and chemical compatibility have been considered (Balashov et al., 2011). Table 1 shows different thermochemical water splitting (TWS) cycle processes and their several properties. The Cu-Cl hybrid cycle has been extensively researched in recent times. Presently, numerous research laboratories and universities continue their investigations. The Cu-Cl cycle has been extensively investigated due to its advantages, which include low

**Table 1**
Some selected types of TWS cycles and their properties.

| TWS types | Reactions | Required energy type for reactions | Temperature | Advantages | Disadvantages |
|---|---|---|---|---|---|
| 4- step Cu-Cl cycle (Ferrandon et al., 2008): (Farsi et al., 2019 | $2CuCl_{2(s)} + H_2O_{(g)} \rightarrow Cu_2OCl_{2(s)} + 2HCl_{(g)}$<br>$Cu_2OCl_{2(s)} \rightarrow 1/2O_{2(g)} + 2CuCl_{(l)}$<br>$CuCl_{2(aq)} \rightarrow CuCl_{2(s)}$<br>$2CuCl_{(aq)} + 2HCl_{(aq)} \rightarrow 2CuCl_{2(aq)} + H_2$ | Heat<br>Heat<br>Work + Heat | 370–400 °C<br>500–530 °C<br><100<br><100 | − Lower operating temperatures<br>− Ability to use low-grade waste heat to improve energy efficiency, and potentially lower cost materials | −Hygroscopic nature of the reactant<br>−Product agglomeration<br>−Multiple side reactions<br>− The need for excess steam for high conversion |
| 4-step Mg-Cl cycle (Ozcan, 2015) | $MgCl_2 + H_2O \rightarrow MgOHCl + HCl_{(aq)}$<br>$MgOHCl \rightarrow MgO + HCl_{(g)}$<br>$MgO + Cl_2 \rightarrow MgCl_2 + 1/2O_2$<br>$2HCl_{(g)} \rightarrow Cl_2 + H_2$ | Heat<br>Heat<br>Work + Heat | 280 °C<br>450 °C<br>450–500 °C<br><100 | −Low temperature<br>− Promising to be integrated with solar and nuclear | −MgO chlorination (Main challenges have been found to be the surface area of the MgO particles and ash layer of $MgCl_2$ on the MgO surface during the reaction.)<br>−Multiple side reactions<br>− Rapid formation of $MgCl_2$ hydrates |
| Fe-Cl cycleUtgikar and Ward, 2006 | $3FeCl_{2(l)} + 4H_2O_{(g)} \rightarrow Fe_3O_{4(s)} + 6HCl_{(g)} + H_{2(g)}$<br>$Fe_3O_{4(s)} + 8HCl_{(g)} \rightarrow FeCl_{2(s)} + 2FeCl_{3(s)} + 4\ H_2O_{(g)}$<br>$2FeCl_{3(g)} \rightarrow 2FeCl_{2(g)} + Cl_{2(g)}$<br>$Cl_{2(g)} + H_2O_{(g)} \rightarrow 2HCl_{(g)} + ½\ O_{2(g)}$ | Heat<br>Heat<br>Heat<br>Heat | 450 °C<br>100 °C<br>300 °C<br>800 °C | −Known thermodynamic<br>− Low cost and abundance of materials<br>−Well known chemistry<br>−inexpensive material price | − Low efficiency<br>− High temperature $FeCl_3$ decomposition<br>− Dimerization of $FeCl_3$ to $Fe_2Cl_6$<br>− High temperature requirement |
| V-Cl cycle (Lewis and Masin, 2009) | $2VCl_{2(s)} + 2HCl_{(l)} \rightarrow 2VCl_{3(s)} + H_{2(g)}$<br>$4VCl_{3(s)} + 2VCl_{4(g)} \rightarrow 2VCl_{2(s)}$<br>$2VCl_{4(l)} \rightarrow 2VCl_3 + Cl_{2(g)}$<br>$Cl_{2(g)} + H_2O_{(g)} \rightarrow 2HCl_{(g)} + 0.5O_{2(g)}$ | Heat<br>Heat<br>Heat<br>Heat | 120 °C<br>766 °C<br>200 °C<br>875 °C | −High efficiency<br>− Low operating cost | −Difficult separations<br>−Slow kinetics<br>−Unknown engineering feasibility<br>−High temperature requiring<br>−High temperature requirement |
| S-I cycle (Fu et al., 2016); ( Mawdsley et al., Aug. 2012) | $H_2SO_{4(g)} \rightarrow H_2O_{(g)} + SO_{2(g)} + 0.5O_2$<br>$O_{2(g)} + 2H_2O_{(l)} + I_{2(l)} \rightarrow H_2SO_{4(l)} + 2HI_{(l)}$<br>$HI_{(g)} \rightarrow I_{2(g)} + H_{2(g)}$ | Heat<br>Heat<br>Heat | 850 °C<br>120 °C<br>300 °C | −Cost effective<br>−Known reaction mechanism | −High temperature $SO_3$ decomposition reaction<br>−Catalyst requirement<br>−Difficulties in gas separation<br>−HI separation |
| HyS cycle (Westinghouse process) (Roeb, 2013); ( Sattler et al., 2017) | $SO_{3(g)} \rightarrow SO_{2(g)} + 1/2O_{2(g)}$<br>$H_2SO_{4(aq)} \rightarrow H_2O_{(g)} + SO_{3(g)}$<br>$2H_2O_{(l)} + SO_{2(g)} \rightarrow H_2SO_{4(aq)} + H_{2(g)}$ | Heat<br>Heat<br>Work | 800 °C<br>450 °C<br>100 °C | −Less water consumption in the electrolysis step<br>−High selectivity<br>−Low cell potential | −Reduction rate of $SO_3$ proceeds slow<br>−High temperature $SO_3$ decomposition reaction |

temperature requirements within the cycle, inexpensive operating costs, and high efficiency.

Numerous hydrogen production methods have been investigated in the literature, such as thermochemical cycles, electrolysis, photoelectrolysis, and photochemistry. These methods provide different approaches for hydrogen production, and each has its own advantages and disadvantages (Olabi, 2023). Hydrogen generation through thermochemical water splitting cycles is a chemical process that splits water into hydrogen and oxygen using either heat alone or a combination of heat and electricity. The hybrid thermochemical cycle uses heat and electricity, while the pure thermochemical cycle solely uses heat to carry out the cycle's reactions. The simplified schematic illustration of the

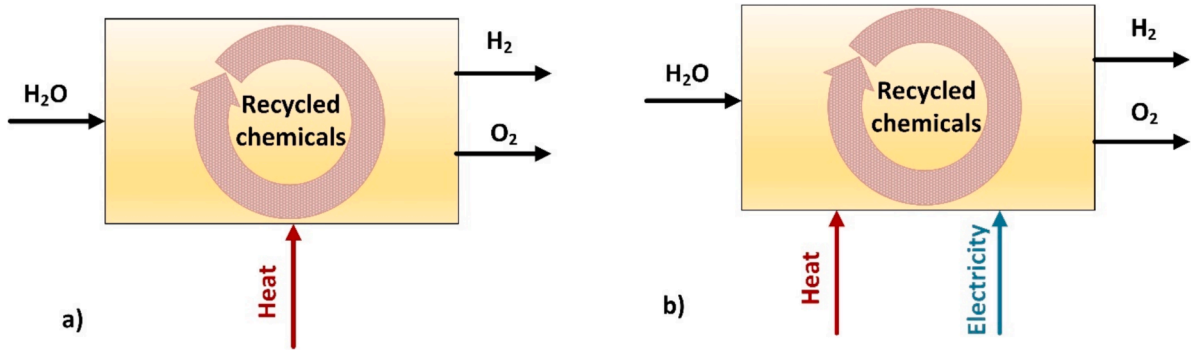



**Fig. 2.** The simplified schematic illustrations of thermochemical water splitting cycles: **a)** pure thermochemical cycle, and **b)** hybrid thermochemical cycle.

thermochemical water splitting cycle is illustrated in Fig. 2. It shows the schematic of hybrid and pure thermochemical cycles. A sequence of reactions occurs within the cycle and water is decomposed into hydrogen and oxygen. The chemicals used in the cycle can be recycled, but the water cannot be recycled (Li et al., 2020). In Cu-Cl cycles, the cycle is completed by using different copper compounds in each reaction step. Each of the reaction steps takes place at a certain temperature. The Cu-Cl thermochemical water splitting cycle is a promising technique for large-scale hydrogen production. The relatively low-grade temperature requirement for the cycle is an important advantage. Due to the low temperature requirement, the heat required in the cycle can also be supplied from waste heat from power plants, solar thermal plants, and nuclear energy. Another important advantage of the Cu-Cl cycle is that the raw materials are inexpensive, and the reaction mechanism is well known.

There are several Cu-Cl configurations in the literature. These configurations can vary based on the number of reaction steps, namely 2, 3, 4, and 5-step thermochemical cycles. The number of reaction steps is a parameter that impacts the performance of the system. Ishaq and Dincer (2019) conducted an assessment study to determine the impacts of various Cu-Cl cycles, namely 3, 4, and 5-step configurations on system performance. They conducted a comparative parametric study to assess the energy and exergy efficiencies of these cycles, using the Aspen Plus for modeling and simulation. The five-step Cu-Cl cycle's energy and exergy efficiencies were 38.8 % and 70.2 %, respectively, according to their findings. In contrast, the three-step cycle exhibited a slightly higher energy efficiency of 39.6 %, but a reduced exergy efficiency of 68.1 %. Nevertheless, the four-step Cu-Cl cycle outperformed both, achieving the highest energy and exergy efficiencies of 41.9 % and 75.7 %, respectively. Their findings indicated that the optimization of thermal management and the reduction of exergy degradation could enhance cycle performance. Table 2 compares these results with results of presented study in terms of energy and exergy efficiencies. Decreasing the number of steps has some disadvantages. Some examples of these disadvantages are high heat requirement, and formation of undesirable side reactions. The comparison of the advantages and disadvantages of Cu-Cl cycles with various configurations is an essential factor in determining the most suited system (Farsi et al., 2019).

In the 1970′s, Dokiya and Kotera (1976) developed a 2-step hybrid Cu-Cl cycle, where the first step was thermal, and the second step was electrolytic. The reaction steps in the cycle are $2CuCl_2 + H_2O \rightarrow 2CuCl + 2HCl + ½\ O_2$ and $2CuCl + 2HCl \rightarrow 2CuCl_2 + H_2$. In the first step, they carried out hydrolysis and decomposition reactions, and in the second step, they carried out the hydrogen production reaction with the electrolysis process. They determined the highest temperature value required for the first step reactions to occur as 600 °C. As a result of the measurements made with the electrolysis they designed for the electrolysis step, they found that the cell voltage was between 0.6–1.0 V.

The required heat could be obtained from different energy resources. Nuclear energy is one of these sources. Al-Zareer et al. (2018) investigated the integration of a Generation IV gas-cooled fast nuclear reactor with a thermochemical Cu-Cl cycle. This system was designed to provide hydrogen and electricity production simultaneously. In the study, hydrogen was produced by thermochemical cracking of water with a four-reaction hybrid Cu-Cl cycle and the produced hydrogen was compressed to reduce the storage volume. They simulated the system using Aspen Plus. According to their simulation results, the energy efficiency of the system was calculated as 14.1 % and the exergy efficiency as 20.7 %. Li et al. (2020) have studied the production of hydrogen by thermochemically splitting water using a hybrid Cu-Cl cycle. Since the highest temperature required in the Cu-Cl cycle is around 530 °C, they emphasized that integration with the Canadian Supercritical Water Reactor (SCWR) or small modular reactors (SMR) could be effective. As part of their research, the electrolysis step of the Cu-Cl cycle was studied at the laboratory scale and the hydrogen production rate was determined as 50 L/h.

Solar-based thermochemical cycles have significant potential to decrease greenhouse gas emissions by providing an environmentally friendly option for large-scale hydrogen production. The Cu-Cl cycle offers a significant opportunity for clean hydrogen generation when integrated with solar energy. Solar energy increases the energy efficiency of these systems while minimizing carbon emissions. Therefore, the solar-driven Cu-Cl cycle is seen as an important step towards building a sustainable hydrogen economy. Ghandehariun et al. (2010) investigated a solar-based five step Cu-Cl thermochemical plant to generate hydrogen. Studies conducted in different locations in Canada have examined solar power plants with various hydrogen production capacities. In these studies, they evaluated the operating parameters of solar fields and storage units for hydrogen production in three different locations (Calgary, Toronto, Sarnia). A mixture of 60 % $NaNO_3$ and 40 % $KNO_3$ was determined as the most suitable molten salt for solar energy storage for the hydrogen generation plant. Studies have shown that a bigger storage unit is needed due to the lower solar radiation in Calgary compared to Toronto and Sarnia during the winter months. In addition, it has been stated that the heat requirement of the oxygen reactor (530 °C) is higher than the heat that can be obtained from existing nuclear power plants, and therefore the use of solar concentrators for the endothermic oxygen reactor has been suggested. The studies also found that for higher hydrogen production rates, the size of the storage tanks increased, and night circulation was necessary to compensate for heat losses from radiation. The results show that solar-assisted thermochemical hydrogen generation of the Cu-Cl cycle is both an efficient and environmentally sustainable method for large-scale applications. Considering energy and economic factors, Coulibaly et al. (2022) developed and examined a new power and hydrogen co-production system. In this study, a three-step Cu-Cl thermochemical cycle

**Table 2**
Comparison of different configurations for Cu-Cl cycle (compiled from (Ishaq and Dincer, 2019)).

| Configuration | Reactions | Temperature | Heat/Work inputs | Energy efficiency | Exergy efficiency |
|---|---|---|---|---|---|
| 3-step | $2Cu_{(s)} + 2HCl_{(g)} \rightarrow 2CuCl_{(l)} + H_{2(g)}$ | 450 °C | Heat | 39.6 % | 68.1 % |
| | $4CuCl_{(s)} \rightarrow 2CuCl_{2(aq)} + 2Cu_{(s)}$ | 30 °C °C | Heat + Work | | |
| | $CuCl_{2(aq)} + H_2O_{(l)} \rightarrow 2CuCl + 2HCl_{(g)} + ½O_{2(g)}$ | 530 °C | Heat | | |
| 4-step | $2CuCl_{(aq)} + 2HCl_{(aq)} \rightarrow 2CuCl_{2(aq)} + H_{2(g)}$ | 25 °C | Heat + Work | 41.9 % | 75.7 % |
| | $Cu_2OCl_{2(s)} \rightarrow 2CuCl_{(l)} + 0.5O_{2(g)}$ | 500 °C | Heat | | |
| | $2CuCl_{2(s)} + H_2O_{(g)} \rightarrow Cu_2OCl_{2(s)} + 2HCl_{(g)}$ | 400 °C | Heat | | |
| | $CuCl_{2(aq)} \rightarrow CuCl_{2(s)}$ | 80 °C | Heat | | |
| 5-step | $2CuCl_{2(s)} + H_2O_{(g)} \rightarrow Cu_2OCl_{2(s)} + 2HCl_{(g)}$ | 400 °C | Heat | 38.8 % | 70.2 % |
| | $Cu_2OCl_{2(s)} \rightarrow 2CuCl_{(l)} + 0.5O_{2(g)}$ | 500 °C | Heat | | |
| | $4CuCl_{(aq)} \rightarrow 2Cu_{(s)} + 2CuCl_{2(aq)}$ | 25 °C | Heat + Work | | |
| | $2Cu_{(s)} + 2HCl_{(g)} \rightarrow 2CuCl_{(l)} + H_{2(g)}$ | 430 °C | Heat | | |
| | $CuCl_{2(aq)} \rightarrow CuCl_{2(s)}$ | 100 °C | Heat | | |
| Present study (3-step cycle) | $2CuCl_{2(s)} + H_2O_{(g)} \rightarrow Cu_2OCl_{2(s)} + 2HCl_{(g)}$ | 370–400 °C | Heat | 72.50 % | 46.70 % |
| | $Cu_2OCl_{2(s)} \rightarrow 2CuCl_{(l)} + 0.5O_{2(g)}$ | 500–530 °C | Heat | | |
| | $2CuCl_{(s)} + 2HCl_{(g)} \rightarrow 2CuCl_{2(s)} + H_{2(g)}$ | 450–500 °C | Heat | | |

produces hydrogen, while a parabolic trough collector power plant and molten carbonate fuel cell (MCFC) generate electricity simultaneously. The molten carbonate fuel cell is the primary element of the system, as it supplies heat to the steam accumulator and the Cu-Cl thermochemical cycle. They conducted a parametric study to evaluate the effect of specific parameters on the system's performance and developed a mathematical model for energy and economic analysis. The calculations indicated that the fuel cell generated 578 GWh of electrical energy, the solar facility generated 25 GWh, and the hydrogen produced was 306 tons. In total, the proposed facility is estimated to have an energy efficiency of 46.80 %. After conducting a parametric analysis, they determined that the energy efficiency of the fuel cell and the Cu-Cl cycle is influenced by the quantity of heat recovered.

The Cu-Cl cycle could be designed as an integrated system that can provide not only hydrogen production but also various energy applications such as power generation, cooling and heat recovery. This system offers a solution that increases energy efficiency and minimizes environmental impacts by combining power generation, cooling and heat recovery. Ouagued et al. (2018) examined the potential of hydrogen production under specific climate conditions by integrating the Cu-Cl thermochemical cycle with a solar parabolic trough system. They performed a comprehensive thermodynamic analysis of the Cu-Cl cycle, considering the energy required for the cycle and the relevant chemical reactions. The Cu-Cl cycle's energy and exergy efficiencies were calculated to be 40.42 % and 92.25 %, respectively, based on the reference conditions. Zhang et al. (2022) presented a novel method to produce hydrogen that integrates a copper-chlorine thermochemical cycle with cascading solar spectral radiation. This system would generate pure hydrogen by utilizing solar energy. They conducted a theoretical analysis of the system's efficiency limits, energy requirements, and the effects of various parameters in their research. The energy demands of the four-step copper-chlorine cycle were simulated using Aspen Plus software. The efficiency of the overall system was assessed through thermodynamic analysis. According to their efficiency analysis, the proposed system exceeded the theoretical limit of single-junction photovoltaic-electrolysis systems by achieving an optimal efficiency of 68.20 %. The efficiency of the actual design was 43.44 %, which was higher than that of systems that did not include a spectrum dividing module. Their research illustrated an efficient approach to improving the cascading utilization of solar energy to generate pure hydrogen energy. Thomas et al. (2020) investigated solid–gas reactions (heterogeneous reaction) to understand the reaction kinetics of the hydrolysis step. They examined the effects of temperature (275 °C-375 °C), reaction time (0–3 h) and vapor mole fraction (0.4–0.9) in the fluidized bed hydrolysis reactor they designed. To prevent possible by-product formation during the reaction, inert gas was sent into the reactor. As a result of their experimental studies, they found that the minimum vapor mole fraction should be 0.5 to prevent the formation of by-product CuCl in the temperature range of 300 °C–325 °C. In addition, as another experimental finding, they found that $Cu_2OCl_2$ was formed at the beginning of the reaction and decomposed into CuO and $CuCl_2$ as the reaction progressed. While they found the activation energy of the hydrolysis reaction of the decomposition of $Cu_2OCl_2$ into $CuCl_2$ and CuO as 44.8 kJ/mol, they calculated the activation energy of the side reaction as 20 kJ/mol. Finally, their experimental studies show that the optimal temperature for high yields of the desired product lies in the range of 300 °C–325 °C, where the minimum vapor mole fraction is 0.5 and the reaction time is 20–40 min.

The Cu-Cl cycle provides several advantages such as low operating temperature requirement between thermochemical water splitting cycles, known chemical reaction mechanisms, high efficiency, and the study of individual reactors and electrolysis steps by many institutions. Its low operating temperature range makes it suitable for integration into nuclear power reactors and solar thermal energy production facilities. While many reaction steps in Cu-Cl cycles require heat input, the hydrogen production step is generally the electrolysis step. The electrolysis reaction step has several disadvantages. Due to the corrosive nature of copper compounds, the materials in the electrolyzer should consist of corrosion-resistant materials. Other disadvantages of the electrolysis step include the need for a membrane, the possibility of copper poisoning on the membranes, and the fact that electricity is more expensive than heat energy. The key contribution of the proposed study is to avoid the economic liability caused by the electrolysis step. The primary goal of this research is to investigate and develop a novel Cu-Cl cycle that operates purely on thermal energy.

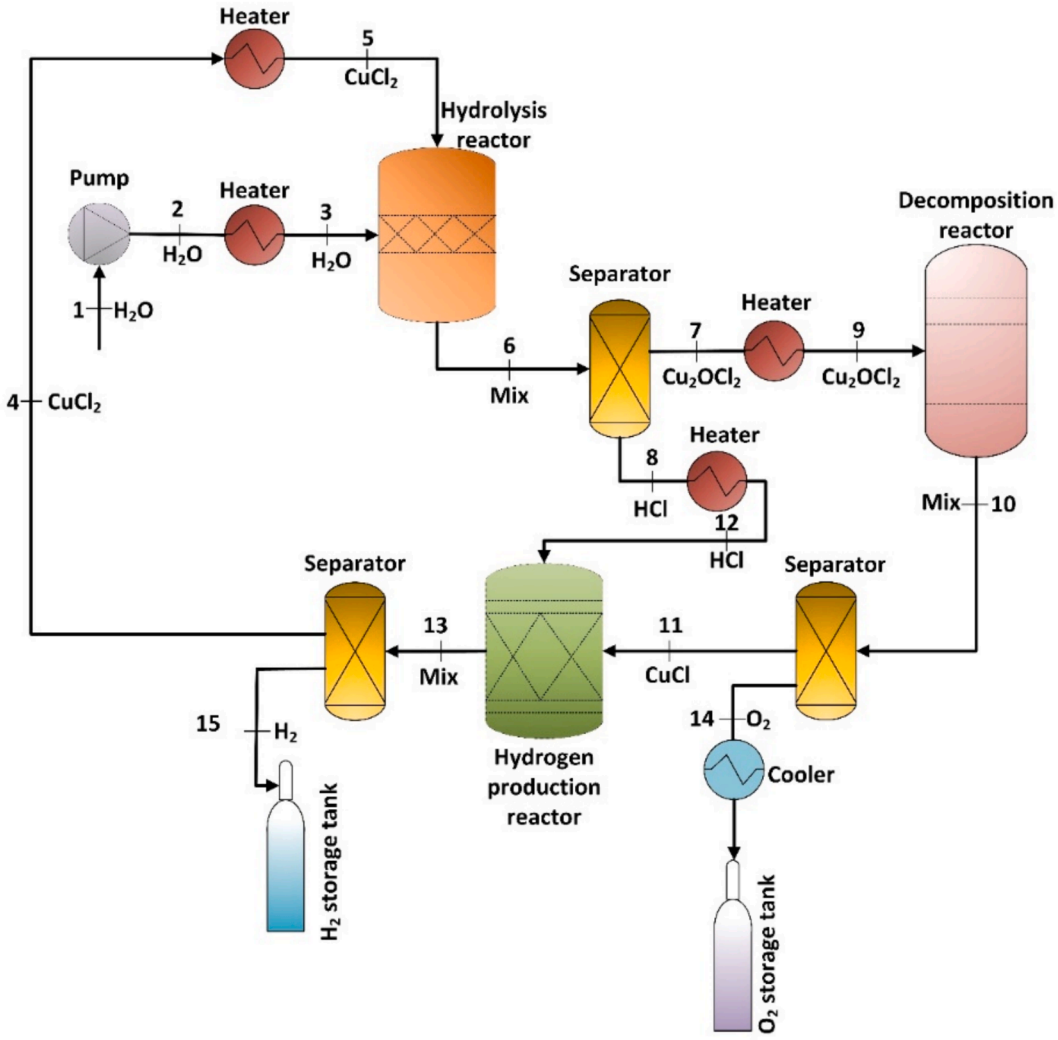
Up until now, presented Cu-Cl studies in the literature are hybrid thermochemical cycles. An electrolyzer is used for the hydrogen production step in the cycle, and hydrogen production occurs by electrochemical reaction. Therefore, the electrolysis step is the main challenge in meeting the performance and cost targets of the Cu-Cl cycle. The elements such as membrane, electrode and catalyst used in the electrolyzer process increase the operating cost of the cycle (Lewis et al., 2009). There are some thermochemical cycles in the literature that are driven entirely by heat input; for example, vanadium-chlorine and iron-chlorine cycles are among such systems. In the context of the Cu-Cl cycle, current studies generally focus on systems that involve a combination of electrical and heat input. Scope of this study, a new Cu-Cl cycle operating entirely with heat energy is presented by eliminating the electrolysis step that increases the cost of the system. The specific objectives of the proposed study are listed below:

- to develop and simulate a novel Cu-Cl thermochemical water splitting cycle that operates entirely using thermal energy input without an electrolysis step in the cycle,
- to conduct parametric studies for the integrated system under various operating conditions, and
- to perform a complete thermodynamic assessment based on energy and exergy efficiencies of the overall system.

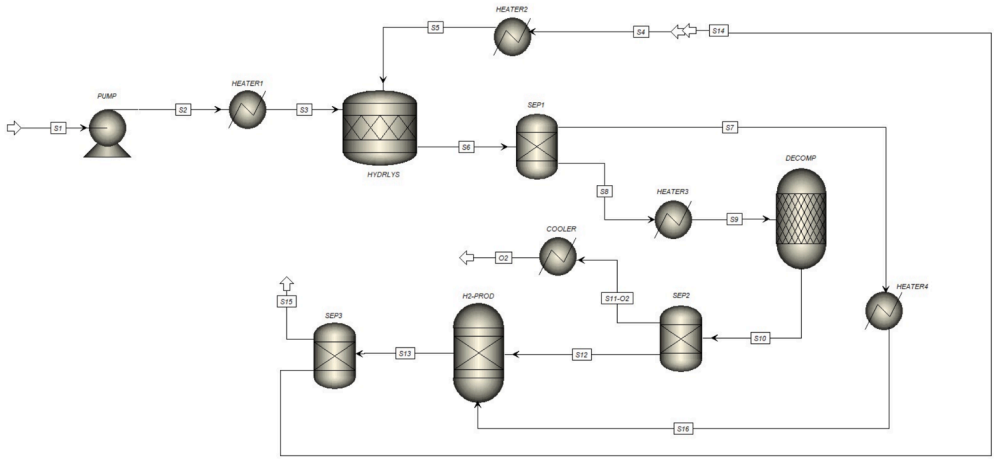
## 2. System Description

The simulation of the presented 3-step entirely thermal energy driven Cu-Cl thermochemical water splitting cycle was performed using the Aspen Plus V14. The Aspen Plus is an industry standard software in chemical process simulations and plays a critical role in modeling, simulation and optimization of complex chemical processes. To simulate Cu-Cl cycle reactions, the R-Stoic reactor model has been used using the stoichiometry of each reactions. Although the stoichiometric mole ratio of water to $CuCl_2$ in the hydrolysis reaction is 0.5, the literature (Lewis et al., 2009) specifies that excess water is required to achieve a high conversion ratio of $Cu_2OCl_2$. Therefore, water is defined as the excess reactant, and $CuCl_2$ is defined as the limiting reactant in the system simulation. There is solid, liquid and gas phases in the system and the interactions of these phases are critical for the correct modeling of the reaction mechanism and thermodynamic equilibrium. For this reason, appropriate property methods for different phases were selected in Aspen Plus simulation. The Solid Model for solid phases, UNIQAC (Universal Quasi-chemical) for liquid phases and Peng-Robinson (Peng-Rob) property methods were used for gas phases.

Both electrical power and heat input are required for the pumps, heaters and reactors in the system, respectively. The absence of an electrolyzer in the proposed system reduces the work input. Only the pumps in the system require work input, while the heaters require heat input. In the calculations, the lower heating value (LHV) of hydrogen is taken as 120,000 kJ/kg $H_2$. While Fig. 3a shows the schematic layout of the system, Fig. 3b shows the Aspen Plus flowsheet of the proposed system. According to the Aspen Plus flowsheet, the water required for the hydrolysis reaction, which is the first reaction of the cycle, is sent to the heater (heater 1) through the pump. The water coming out of the heater at 400 °C is introduced into the hydrolysis reactor as steam. The other reactant of the hydrolysis reaction, $CuCl_2$ (S4), is sent to the hydrolysis reactor after being heated to 400 °C in heater (heater 2). The




(a)




(b)

**Fig. 3.** Two diagrams: (a) a schematic layout of the designed system and (b) the Aspen Plus flowsheet of the simulated Cu-Cl cycle.

hydrolysis reactor generates products after steam and $CuCl_2$ react. The separator (SEP1) separates these products into HCl gas and $Cu_2OCl_2$ solids. Since the decomposition reaction of $Cu_2OCl_2$ occurs at 530 °C, $Cu_2OCl_2$ (S8) is sent to the heater (heater 3) before entering the decomposition reactor.

In the decomposition reactor, $Cu_2OCl_2$ decomposes at 530 °C to produce $O_2$ (S11) and CuCl (S12). The products are sent to the separator (SEP 2) to be separated. Since the released oxygen will not be used again in the cycle, it is removed from the cycle. In the third step of the cycle, which is the hydrogen production step, HCl gas (S16) and CuCl (S12)

react at 500 °C to form $CuCl_2$ (S14) and $H_2$ (S15). Thus, the cycle is completed.

## 3. Modelling and analysis

A three-step Cu-Cl cycle, that operates entirely with thermal energy input, was simulated using the Aspen Plus. This study examines the thermodynamic aspects of the system by applying the first and second laws of thermodynamics. The Engineering Equation Solver (EES) was utilized while performing the thermodynamic analysis of the system. Several sensitivity analyses are conducted based on the quantities of reactants, reaction temperatures, and the ratio of steam/$CuCl_2$ in the proposed cycle. Several assumptions are made while performing the analyses of the presented system, and they are listed below:

- The reference ambient temperature ($T_0$) and pressure are 25 °C and 100 kPa, respectively.
- The potential and kinetic energy changes are neglected in the system.
- Each reaction is assumed as in steady state and adiabatic in the system.
- The isentropic efficiency is assumed to be 85 % for the pump.

### 3.1. Thermodynamic analysis of the Cu-Cl cycle

The mass, energy, entropy, and exergy balance equations are employed to analyze the components involved in the cycle. The equations for each component are presented below.

#### 3.1.1. Hydrolysis reactor

The first reaction step of the cycle is the hydrolysis reaction of $CuCl_2$. The reaction takes place at atmospheric pressure and in the temperature range of 370–400 °C. One of the reactants, $H_2O$, is heated to 400 °C before entering the reactor, and in the same manner, the $CuCl_2$ solid is heated to the reaction temperature and sent to the reactor. $Cu_2OCl_2$ and HCl gas are final products of the hydrolysis reaction. For the hydrolysis reactor, the mass balance equations (MBE), energy balance equations (EBE), entropy balance equations (EnBE), and exergy balance equations (ExBE) can be written as follows, respectively:

$$\mathrm{MBE}: \dot{m}_{s3} + \dot{m}_{s5} = \dot{m}_{s6} \tag{1}$$

$$\mathrm{EBE}: \dot{m}_{s3}h_{s3} + \dot{m}_{s5}h_{s5} + \dot{Q}_{Hyd} = \dot{m}_{s6}h_{s6} \tag{2}$$

$$\mathrm{EnBE}: \dot{m}_{s3}s_{s3} + \dot{m}_{s5}s_{s5} + \frac{\dot{Q}_{Hyd}}{T_b} + \dot{S}_{gen,Hyd} = \dot{m}_{s6}s_{s6} \tag{3}$$

$$\mathrm{ExBE}: \dot{m}_{s3}ex_{s3} + \dot{m}_{s5}ex_{s5} + \dot{E}x_{\dot{Q}_{Hyd}} = \dot{m}_{s6}ex_{s6} + \dot{E}x_{dest,Hyd} \tag{4}$$

The energy, entropy, and exergy chemical balance equations for the hydrolysis reaction could be written as below:

$$2CuCl_{2(s)} + H_2O_{(g)} \rightarrow Cu_2OCl_{2(s)} + 2HCl_{(g)} \tag{5}$$

$$\mathrm{MBE}: \dot{n}_{CuCl_2} + \dot{n}_{H_2O} = \dot{n}_{Cu_2OCl_2} + \dot{n}_{HCl} \tag{6}$$

$$\begin{aligned}\mathrm{EBE}: &\ \dot{n}_{CuCl_2}\left(\overline{h}_f^0 + \overline{h} - \overline{h}^0 - P\overline{v}\right)_{CuCl_2} + \dot{n}_{H_2O}\left(\overline{h}_f^0 + \overline{h} - \overline{h}^0 - P\overline{v}\right)_{H_2O} + \dot{Q}_{in} \\ &= \dot{n}_{Cu_2OCl_2}\left(\overline{h}_f^0 + \overline{h} - \overline{h}^0 - P\overline{v}\right)_{Cu_2OCl_2} + \dot{n}_{HCl}\left(\overline{h}_f^0 + \overline{h} - \overline{h}^0 - P\overline{v}\right)_{HCl}\end{aligned} \tag{7}$$

$$\begin{aligned}\mathrm{EnBE}: &\ \dot{n}_{CuCl_2}\left(\overline{s}_f^0 + \overline{s} - \overline{s}^0 - P\overline{v}\right)_{CuCl_2} + \dot{S}_{gen} + \frac{\dot{Q}_{in}}{T_s} + \dot{n}_{H_2O}\left(\overline{s}_f^0 + \overline{s} - \overline{s}^0 - P\overline{v}\right)_{H_2O} \\ &= \dot{n}_{Cu_2OCl_2}\left(\overline{s}_f^0 + \overline{s} - \overline{s}^0 - P\overline{v}\right)_{Cu_2OCl_2} + \dot{n}_{HCl}\left(\overline{s}_f^0 + \overline{s} - \overline{s}^0 - P\overline{v}\right)_{HCl}\end{aligned} \tag{8}$$

$$\begin{aligned}\mathrm{ExBE}:: &\ \dot{n}_{CuCl_2}\left(\overline{ex}_f^0 + \overline{ex} - \overline{ex}^0 - P\overline{v}\right)_{CuCl_2} + \dot{Q}_{in}\left(1 - \frac{T_0}{T_s}\right) + \dot{n}_{H_2O} \\ &\left(\overline{ex}_f^0 + \overline{ex} - \overline{ex}^0 - P\overline{v}\right)_{H_2O} = \dot{n}_{Cu_2OCl_2}\left(\overline{ex}_f^0 + \overline{ex} - \overline{ex}^0 - P\overline{v}\right)_{Cu_2OCl_2} \\ &+ \dot{n}_{HCl}\left(\overline{ex}_f^0 + \overline{ex} - \overline{ex}^0 - P\overline{v}\right)_{HCl} + \dot{E}x_d\end{aligned} \tag{9}$$

In eq. (9), specific exergy of stream is $\overline{ex} = \left(\overline{h} - \overline{h}^0\right) - T_0\left(\overline{s} - \overline{s}^0\right) + \overline{ex}^{CH}$, and $ex = (h - h_0) - T_0\,(s - s_0)$.

#### 3.1.2. Decomposition reactor

The second reaction step of the cycle is the decomposition reaction of $Cu_2OCl_2$ into $O_2$ and CuCl which is shown in eq. (14). The reaction occurs at atmospheric pressure and temperature range of 500–530 °C. The mass, energy, entropy, and exergy balance equations for the decomposition reactor could be expressed as follows, respectively:

$$\mathrm{MBE}: \dot{m}_{s9} = \dot{m}_{s10} = \dot{m} \tag{10}$$

$$\mathrm{EBE}: \dot{m}_{s9}h_{s9} + \dot{Q}_{Dec} = \dot{m}_{s10}h_{s10} \tag{11}$$

$$\mathrm{EnBE}: \dot{m}_{s9}s_{s9} + \frac{\dot{Q}_{Dec}}{T_b} + \dot{S}_{gen,Dec} = \dot{m}_{s10}s_{s10} \tag{12}$$

$$\mathrm{ExBE}: \dot{m}_{s9}ex_{s9} + \dot{E}x_{\dot{Q}_{Dec}} = \dot{m}_{s10}ex_{s10} + \dot{E}x_{dest,\,Dec} \tag{13}$$

The energy, entropy, and exergy chemical balance equations for the decomposition of the $Cu_2OCl_2$ into CuCl and $O_2$ reaction could be written as follows:

$$Cu_2OCl_{2(s)} \rightarrow 2CuCl_{(l)} + 0.5O_{2(g)} \tag{14}$$

$$\mathrm{MBE}: \dot{n}_{Cu_2OCl_2} = \dot{n}_{CuCl} + \dot{n}_{O_2} \tag{15}$$

$$\begin{aligned}\mathrm{EBE}: &\ \dot{n}_{Cu_2OCl_2}\left(\overline{h}_f^0 + \overline{h} - \overline{h}^0 - P\overline{v}\right)_{Cu_2OCl_2} + \dot{Q}_{in} \\ &= \dot{n}_{CuCl}\left(\overline{h}_f^0 + \overline{h} - \overline{h}^0 - P\overline{v}\right)_{CuCl} + \dot{n}_{O_2}\left(\overline{h}_f^0 + \overline{h} - \overline{h}^0 - P\overline{v}\right)_{O_2}\end{aligned} \tag{16}$$

$$\begin{aligned}\mathrm{EnBE}: &\ \dot{n}_{Cu_2OCl_2}\left(\overline{s}_f^0 + \overline{s} - \overline{s}^0 - P\overline{v}\right)_{Cu_2OCl_2} + \dot{S}_{gen} + \frac{\dot{Q}_{in}}{T_s} \\ &= \dot{n}_{CuCl}\left(\overline{s}_f^0 + \overline{s} - \overline{s}^0 - P\overline{v}\right)_{CuCl} + \dot{n}_{O_2}\left(\overline{s}_f^0 + \overline{s} - \overline{s}^0 - P\overline{v}\right)_{O_2}\end{aligned} \tag{17}$$

$$\begin{aligned}\mathrm{ExBE}: &\ \dot{n}_{Cu_2OCl_2}\left(\overline{ex}_f^0 + \overline{ex} - \overline{ex}^0 - P\overline{v}\right)_{Cu_2OCl_2} + \dot{Q}_{in}\left(1 - \frac{T_0}{T_s}\right) \\ &= \dot{n}_{CuCl}\left(\overline{ex}_f^0 + \overline{ex} - \overline{ex}^0 - P\overline{v}\right)_{CuCl} + \dot{n}_{O_2}\left(\overline{ex}_f^0 + \overline{ex} - \overline{ex}^0 - P\overline{v}\right)_{O_2} + \dot{E}x_d\end{aligned} \tag{18}$$

#### 3.1.3. Hydrogen production reactor

The last reaction step of the cycle is the hydrogen generation reaction. The reaction takes place at atmospheric pressure and in the temperature range of 450–500 °C. The HCl gas produced in the hydrolysis reaction step and the CuCl solid produced in the decomposition step react to form hydrogen gas and $CuCl_2$. For the hydrogen production reactor, the mass, energy, entropy, and exergy balance equations could be given as follows, respectively:

$$\mathrm{MBE}: \dot{m}_{s12} + \dot{m}_{s16} = \dot{m}_{s13} \tag{19}$$

$$\text{EBE}: \dot{m}_{s12}h_{s12} + \dot{m}_{s16}h_{s16} + \dot{Q}_{H_{2prod}} = \dot{m}_{s13}h_{s13} \tag{20}$$

$$\text{EnBE}: \dot{m}_{s12}s_{s12} + \dot{m}_{s16}s_{s16} + \frac{\dot{Q}_{H_{2prod}}}{T_b} + \dot{S}_{gen,H_{2prod}} = \dot{m}_{s13}s_{s13} \tag{21}$$

$$\text{ExBE}: \dot{m}_{s12}ex_{12} + \dot{m}_{s16}ex_{s16} + \dot{E}x_{\dot{Q}_{H_{2prod}}} = \dot{m}_{s13}ex_{s13} + \dot{E}x_{dest,Hyd} \tag{22}$$

The energy, entropy, and exergy chemical balance equations for the hydrogen production reaction could be written as follows:

$$2CuCl_{(s)} + 2HCl_{(g)} \rightarrow 2CuCl_{2(s)} + H_2 \tag{23}$$

$$\text{MBE}: \dot{n}_{CuCl} + \dot{n}_{H_2O} = \dot{n}_{Cu_2OCl_2} + \dot{n}_{HCl} \tag{24}$$

$$\begin{aligned}\text{EBE}:: \dot{n}_{CuCl}\left(\overline{h}_f^0 + \overline{h} - \overline{h}^0 - P\overline{v}\right)_{CuCl} + \dot{n}_{HCl}\left(\overline{h}_f^0 + \overline{h} - \overline{h}^0 - P\overline{v}\right)_{HCl} + \dot{Q}_{in} \\ = \dot{n}_{CuCl_2}\left(\overline{h}_f^0 + \overline{h} - \overline{h}^0 - P\overline{v}\right)_{CuCl_2} + \dot{n}_{H_2}\left(\overline{h}_f^0 + \overline{h} - \overline{h}^0 - P\overline{v}\right)_{H_2}\end{aligned} \tag{25}$$

$$\begin{aligned}\text{EnBE}: \dot{n}_{CuCl}\left(\overline{s}_f^0 + \overline{s} - \overline{s}^0 - P\overline{v}\right)_{CuCl} + \dot{S}_{gen} + \frac{\dot{Q}_{in}}{T_s} + \dot{n}_{HCl}\left(\overline{s}_f^0 + \overline{s} - \overline{s}^0 - P\overline{v}\right)_{HCl} \\ = \dot{n}_{CuCl_2}\left(\overline{s}_f^0 + \overline{s} - \overline{s}^0 - P\overline{v}\right)_{CuCl_2} + \dot{n}_{H_2}\left(\overline{s}_f^0 + \overline{s} - \overline{s}^0 - P\overline{v}\right)_{H_2}\end{aligned} \tag{26}$$

$$\begin{aligned}\text{ExBE}: \ :\dot{n}_{CuCl}\left(\overline{ex}_f^0 + \overline{ex} - \overline{ex}^0 - P\overline{v}\right)_{CuCl} + \dot{Q}_{in}\left(1 - \frac{T_0}{T_s}\right) + \dot{n}_{HCl} \\ \left(\overline{ex}_f^0 + \overline{ex} - \overline{ex}^0 - P\overline{v}\right)_{HCl} = \dot{n}_{CuCl_2}\left(\overline{ex}_f^0 + \overline{ex} - \overline{ex}^0 - P\overline{v}\right)_{CuCl_2} + \dot{n}_{H_2} \\ \left(\overline{ex}_f^0 + \overline{ex} - \overline{ex}^0 - P\overline{v}\right)_{H_2} + \dot{E}x_d\end{aligned} \tag{27}$$

### 3.1.4. Separators

The products are transferred from the reactors to the separator for separation. The balance equations of the three separators used in the cycle are as follows:

For separator 1:

$$\text{MBE}: \dot{m}_{s6} = \dot{m}_{s7} + \dot{m}_{s8} \tag{28}$$

$$\text{EBE}: \dot{m}_{s6}h_{s6} + \dot{Q}_{sep1} = \dot{m}_{s7}h_{s7} + \dot{m}_{s8}h_{s8} \tag{29}$$

$$\text{EnBE}: \dot{m}_{s6}s_{s6} + \frac{\dot{Q}_{sep1}}{T_b} + \dot{S}_{gen,sep1} = \dot{m}_{s7}s_{s7} + \dot{m}_{s8}s_{s8} \tag{30}$$

$$\text{ExBE}: \dot{m}_{s6}ex_{s6} + \dot{E}x_{\dot{Q}_{sep1}} = \dot{m}_{s7}ex_{s7} + \dot{m}_{s8}ex_{s8} + \dot{E}x_{dest,\ sep1} \tag{31}$$

For separator 2:

$$\text{MBE}: \dot{m}_{s10} = \dot{m}_{s11} + \dot{m}_{s12} \tag{32}$$

$$\text{EBE}: \dot{m}_{s10}h_{s10} + \dot{Q}_{sep2} = \dot{m}_{s11}h_{s11} + \dot{m}_{s12}h_{s12} \tag{33}$$

$$\text{EnBE}: \dot{m}_{s10}s_{s10} + \frac{\dot{Q}_{sep2}}{T_b} + \dot{S}_{gen,sep2} = \dot{m}_{s11}s_{s11} + \dot{m}_{s12}s_{s12} \tag{34}$$

$$\text{ExBE}: \dot{m}_{s10}ex_{s10} + \dot{E}x_{\dot{Q}_{sep2}} = \dot{m}_{s11}ex_{s11} + \dot{m}_{s12}ex_{s12} + \dot{E}x_{dest,\ sep2} \tag{35}$$

For separator 3:

$$\text{MBE}: \dot{m}_{s13} = \dot{m}_{s14} + \dot{m}_{s15} \tag{36}$$

$$\text{EBE}: \dot{m}_{s13}h_{s13} + \dot{Q}_{sep3} = \dot{m}_{s14}h_{s14} + \dot{m}_{s15}h_{s15} \tag{37}$$

$$\text{EnBE}: \dot{m}_{s13}s_{s13} + \frac{\dot{Q}_{sep3}}{T_b} + \dot{S}_{gen,sep3} = \dot{m}_{s14}s_{s14} + \dot{m}_{s15}s_{s15} \tag{38}$$

$$\text{ExBE}: \dot{m}_{s13}ex_{s13} + \dot{E}x_{\dot{Q}_{sep3}} = \dot{m}_{s14}ex_{s14} + \dot{m}_{s15}ex_{s15} + \dot{E}x_{dest,\ sep3} \tag{39}$$

### 3.1.5. Heaters and pump

There is a temperature required for each reaction to occur in the reactors. Before the reactants are sent to the reactor, they are set to this reaction temperature and sent to the reactor. A pump is used to send the water used in the system to the heater. The balance equations of the pumps and heaters could be written as follows:

For pump:

$$\text{MBE}: \dot{m}_{s1} = \dot{m}_{s2} = \dot{m} \tag{40}$$

$$\text{EBE}: \dot{m}_{s1}h_{s1} + \dot{W}_p = \dot{m}_2h_2 \tag{41}$$

$$\text{EnBE}: \dot{m}_{s1}s_{s1} + \dot{S}_{gen,p} = \dot{m}_2s_2 \tag{42}$$

$$\text{ExBE}: \dot{m}_{s1}ex_{s1} + \dot{W}_p = \dot{m}_{s2}ex_{s2} + \dot{E}x_{dest,p} \tag{43}$$

For heater 1:

$$\text{MBE}: \dot{m}_{s2} = \dot{m}_{s3} = \dot{m} \tag{44}$$

$$\text{EBE}: \dot{m}_{s2}h_{s2} + \dot{Q}_{heater1} = \dot{m}_{s3}h_{s3} \tag{45}$$

$$\text{EnBE}: \dot{m}_{s2}s_{s2} + \frac{\dot{Q}_{heater1}}{T_b} + \dot{S}_{gen,heater1} = \dot{m}_{s3}s_{s3} \tag{46}$$

$$\text{ExBE}: \dot{m}_{s2}ex_{s2} + \dot{E}x_{\dot{Q}_{heater1}} = \dot{m}_{s3}ex_{s3} + \dot{E}x_{dest,\ heater1} \tag{47}$$

For heater 2:

$$\text{MBE}: \dot{m}_{s4} = \dot{m}_{s5} = \dot{m} \tag{48}$$

$$\text{EBE}: \dot{m}_{s4}h_{s4} + \dot{Q}_{heater2} = \dot{m}_{s5}h_{s5} \tag{49}$$

$$\text{EnBE}: \dot{m}_{s4}s_{s4} + \frac{\dot{Q}_{heater2}}{T_b} + \dot{S}_{gen,heater2} = \dot{m}_{s5}s_{s5} \tag{50}$$

$$\text{ExBE}: \dot{m}_{s4}ex_{s4} + \dot{E}x_{\dot{Q}_{heater2}} = \dot{m}_{s5}ex_{s5} + \dot{E}x_{dest,\ heater2} \tag{51}$$

For heater 3:

$$\text{MBE}: \dot{m}_{s8} = \dot{m}_{s9} = \dot{m} \tag{52}$$

$$\text{EBE}: \dot{m}_{s8}h_{s8} + \dot{Q}_{heater3} = \dot{m}_{s9}h_{s9} \tag{53}$$

$$\text{EnBE}: \dot{m}_{s8}s_{s8} + \frac{\dot{Q}_{heater3}}{T_b} + \dot{S}_{gen,heater3} = \dot{m}_{s9}s_{s9} \tag{54}$$

$$\text{ExBE}: \dot{m}_{s8}ex_{s8} + \dot{E}x_{\dot{Q}_{heater3}} = \dot{m}_{s9}ex_{s9} + \dot{E}x_{dest,\ heater3} \tag{55}$$

For heater 4:

$$\text{MBE}: \dot{m}_{s7} = \dot{m}_{s16} = \dot{m} \tag{56}$$

$$\text{EBE}: \dot{m}_{s7}h_{s7} + \dot{Q}_{heater4} = \dot{m}_{s16}h_{s16} \tag{57}$$

$$\text{EnBE}: \dot{m}_{s7}s_{s7} + \frac{\dot{Q}_{heater4}}{T_b} + \dot{S}_{gen,heater4} = \dot{m}_{s16}s_{s16} \tag{58}$$

$$\text{ExBE}: \dot{m}_{s7}ex_{s7} + \dot{E}x_{\dot{Q}_{heater4}} = \dot{m}_{s16}ex_{s16} + \dot{E}x_{dest,\ heater4} \tag{59}$$

Energy and exergy efficiencies of the overall system

The formulations used to determine the system's total energy and exergy efficiencies are as follows:

$$\eta = \frac{\dot{m}_{H_2}LHV_{H_2}}{\dot{Q}_{net,in} + \dot{W}_e} \tag{60}$$

and

$$\Psi = \frac{\dot{m}_{H_2} ex_{H_2}}{\dot{E}x_{\dot{Q}_{net,in}} + \dot{W}_e} \quad (61)$$

where $\dot{W}_e$ represents the pump work in the system. The system does not include an electrolysis step. For this reason, there are no additional electrical requirements except a pump. Also, $\dot{Q}_{net,in}$ represents the summation of all heat duties in the system as written as follows:

$$\dot{Q}_{net,in} = \dot{Q}_{pre-heaters} + \dot{Q}_{hyd\ reactor} + \dot{Q}_{dec\ reactor} + \dot{Q}_{H_2 reactor} \quad (62)$$

## 4. Chemical exergy analysis

The exergy of a process at a given state is the sum of its physical and chemical exergy components. For this reason, the total exergy of a system is calculated thermodynamically by combining the physical exergy resulting from physical state changes with the chemical exergy resulting from chemical reactions, and this relationship is given below:

$$ex = ex_{ph} + ex_{ch} \quad (63)$$

The correlation for chemical exergy and physical exergy can be written as follows:

$$ex_{ch} = \sum x_j ex_{ch}^0 + RT_0 \sum x_j \ln(x_j) \quad (64)$$

$$ex_{ph} = h - h_0 - T_0(s - s_0) \quad (65)$$

where $x_j$, $ex_{ch}^0$ and R represent mole fraction of compound or element j, standard specific chemical exergy of the compound or element j, universal gas constant, respectively. Standard chemical exergy and standard Gibbs free energy of formation are based on a typical environmental condition where the ambient temperature ($T_0$) is 25 °C and the ambient pressure ($P_0$) is 1 atm. The standard Gibbs free energy of formation and specific chemical exergy values for reactants and products are taken from the literature and are given in Table 3. If a substance is not present in the environment, to find the standard chemical exergy of this substance, the reaction of the substance with other substances whose standard chemical exergies are known is considered, and this correlation can be written as follows:

$$\overline{ex}^{ch} = -\Delta G + \sum_P n\overline{ex}^{ch} - \sum_R n\overline{ex}^{ch} \quad (66)$$

where $\Delta G$ and n represent the change in Gibbs function for a specific reaction and the moles of reactants-products, respectively.

## 5. Results and discussion

In this study, thermophysical properties important for a particular process were obtained through the Aspen Plus. In the simulation, some parameters such as temperature, pressure, mole flow rate, molar enthalpy, molar entropy, and molar exergy were calculated for various fluids and substances and are shown in Table 4. These data are important for the thermodynamic analysis of the system and the evaluation of reactor performances. The data in the table are used in balance equations, energy efficiency and exergy efficiency calculations of the system. In Fig. 4, the effect of $CuCl_2$ used as a reactant in the hydrolysis reaction on the products formed was investigated. According to the graph, as the molar flow of $CuCl_2$ increases, a linear increase is observed in both $Cu_2OCl_2$ and $H_2$ molar flows. When the general conversion rate of $CuCl_2$ in the hydrolysis reaction is considered, the difference between these products shows that $Cu_2OCl_2$ is produced at a higher molar rate. Furthermore, this graph reveals that the amount of $CuCl_2$ used as a reactant increases the production of both $Cu_2OCl_2$ and $H_2$, and the product distribution of the reaction can be controlled depending on the molar flow of this reactant. Another reactant is water in the Cu-Cl cycle. Water is sent to the hydrolysis reactor as steam and the steam reacts with solid $CuCl_2$ particles. To enhance the $Cu_2OCl_2$ conversion ratio and hence boost $H_2$ production, it is advisable to introduce excess water into the reactor, particularly during the hydrolysis process. Excess water contributes to the complete contact of the reactants in the reaction medium, ensuring that the reaction no longer limits the reactants. This situation increases the conversion rate of $Cu_2OCl_2$ in the hydrolysis reaction and provides higher product yield. In addition, the increase in $Cu_2OCl_2$ conversion directly leads to an increase in $H_2$ production. In this context, excess water accelerates the reaction kinetics, ensures that the hydrolysis step occurs more effectively and as a result, increases the efficiency of the Cu- Cl cycle. Therefore, excess water in the hydrolysis phase is an important factor in terms of both $Cu_2OCl_2$ and $H_2$ production, and controlling the optimal amount of water can positively affect the overall performance of the process. In this context, the effect of $H_2O$ mole flow rate on the produced $Cu_2OCl_2$ mole flow rate and the thermal load on the first heater is investigated in Fig. 5. While the horizontal axis shows the $H_2O$ mole flow (kmol/h), the left vertical axis shows the produced $Cu_2OCl_2$ mole flow (kmol/h), and the right vertical axis shows the thermal load (kW) of heater 1. In the graph, it is observed that the increase in the $H_2O$ mole flow rate causes a linear increase in both the $Cu_2OCl_2$ production and the thermal load on the heater. It is found that with the increase in the $H_2O$ mole flow, the $Cu_2OCl_2$ production increases and the thermal load on the heater increases in parallel. This linear relationship shows that increasing the amount of water in the system positively affects the reaction kinetics and increases the energy demand of the process. As a result, increasing the amount of water in the hydrolysis step stands out as a critical parameter that directly affects both product yield and energy demand.

The effects of $Cu_2OCl_2$ mole flow rate on the produced CuCl, $O_2$ and $H_2$ mole flows are further investigated in Fig. 6. This graph helps us to better understand the reaction efficiency and product distribution in the Cu-Cl thermochemical cycle by revealing the effects of $Cu_2OCl_2$ mole flow rate on the produced CuCl, $O_2$ and $H_2$. It is observed that the increase in $Cu_2OCl_2$ mole flow initially leads to a linear increase in the mole flows of all products. It is observed that there is a regular increase in the production of CuCl and $O_2$, but the production of $H_2$ remains constant after a certain point. This shows that after a certain flow rate of $Cu_2OCl_2$, there is no limiting effect on the production of $H_2$, and the maximum production is reached. As a result, the production of CuCl and $O_2$ increased continuously with the increase of $Cu_2OCl_2$ molar flow rate, while the production of $H_2$ was fixed at a certain level. The impact of different reaction temperatures (350 °C – 550 °C) on the heat duty of three different reactors (hydrolysis, decomposition, and $H_2$ production reactors) in the Cu-Cl cycle were investigated in Fig. 7. According to the findings observed in the graph, the thermal load of the decomposition reactor was at the highest level in each temperature range and was fixed at approximately 0.22 kW, especially starting from 400 °C.

The heat duty of the $H_2$ production reactor also increased proportionally with temperature and reached a value of approximately 0.125 kW after 400 °C. The thermal load of the hydrolysis reactor remained at lower levels than the other two reactors and showed a very limited change with the increase in temperature. As a result of this study, it was

**Table 3**
The standard chemical exergy and specific Gibbs free energy of formation values at environmental conditions (compiled from (Zamfirescu et al., 2010).

| Compounds/ Elements | Standard chemical exergy (kJ/mol) | Specific Gibbs free energy of formation (kJ/mol) |
|---|---|---|
| $H_2O_{(g)}$ | −228,638 | 9437 |
| $H_2O_{(l)}$ | −237,170 | 920 |
| $CuCl_{2(s)}$ | −161,689 | 945,10 |
| $HCl_{(g)}$ | −95,296 | 84,549 |
| $CuO_{(s)}$ | −128,312 | 6273 |
| $CuCl_{(l)}$ | −115,994 | 78,406 |
| $CuCl_{(s)}$ | −120,884 | 73,516 |
| $H_2$ | 236,090 | 0 |
| $O_2$ | 19.3 | 0 |

**Table 4**
The thermophysical property table of the proposed system.

| State Point | Stream | Mol Flow Rate (kmol/h) | Temperature (°C) | Pressure (kPa) | Molar enthalpy (kJ/kmol) | Molar entropy (kJ/kmolK) | Molar exergy (kJ/kmol) |
|---|---|---|---|---|---|---|---|
| S1 | $H_2O$ | 0.0017 | 25 | 100 | −285800.16 | −163.14 | 0 |
| S2 | $H_2O$ | 0.0017 | 25 | 3000 | −285741.83 | −162.94 | 0.32 |
| S3 | $H_2O$ | 0.0017 | 400 | 100 | −226755.34 | −13.19 | 14337.99 |
| S4 | $CuCl_2$ | 0.0058 | 25 | 100 | −205850 | −148.08 | 0 |
| S5 | $CuCl_2$ | 0.0058 | 400 | 100 | −173250.53 | −80.64 | 12491.19 |
| S6 | $Cu_2OCl_2$ /HCl/ $CuCl_2$ | 0.0075 | 400 | 100 | −178564.74 | 284.43 | 5869.23 |
| S7 | HCl/ CuCl | 0.0035 | 400 | 100 | −81321.79 | 42.31 | 4689.09 |
| S8 | $Cu_2OCl_2$/HCl/$CuCl_2$ | 0.0040 | 400 | 100 | −261915.84 | 491.96 | 6876.64 |
| S9 | $Cu_2OCl_2$/$CuCl_2$/HCl | 0.0040 | 530 | 100 | −258371.40 | 496.61 | 9035.38 |
| S10 | CuCl/$O_2$ HCl/$CuCl_2$ | 0.0066 | 530 | 100 | −28445.88 | 39.68 | 27829.54 |
| S11 | $O_2$ | 0.0010 | 530 | 100 | 17462.24 | 34.41 | 8052.75 |
| S12 | CuCl/HCl/$CuCl_2$ | 0.0057 | 530 | 100 | −35540.04 | 40.36 | 30876.02 |
| S13 | $CuCl_2$/$H_2$/HCl/$Cu_2OCl_2$ | 0.0074 | 500 | 100 | −127204.79 | −47.23 | 12664.82 |
| S14 | $CuCl_2$/HCl/$Cu_2OCl_2$ | 0.0058 | 500 | 100 | −168515.54 | −69.71 | 14739.14 |
| S15 | $H_2$ | 0.0017 | 500 | 100 | 13904.54 | 27.96 | 5567.01 |
| S16 | $Cu_2OCl_2$/HCl | 0.0035 | 500 | 100 | −79819.75 | 44.32 | 5592.36 |

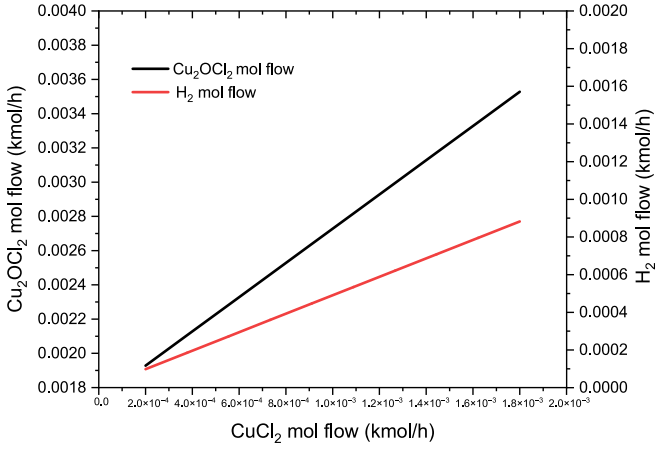



**Fig. 4.** The effect of varying $CuCl_2$ mole flow rate on the $Cu_2OCl_2$ and $H_2$ mole flow.

revealed that the decomposition reactor had the highest thermal load requirement with temperature, while the hydrolysis reactor showed a lower energy demand. The thermodynamic requirements of the chemical reactions taking place in each reactor are different from each other in Fig. 8. The heat duty depends not only on the increase in temperature,

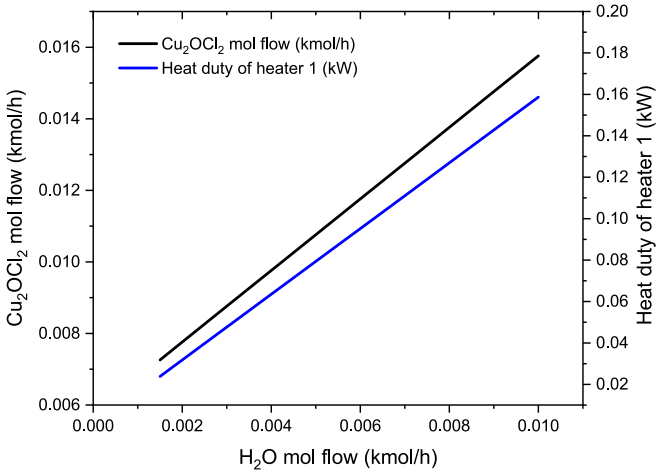



**Fig. 5.** The effect of varying $H_2O$ mole flow rate on the $Cu_2OCl_2$ produced and heat duty of heater 1.

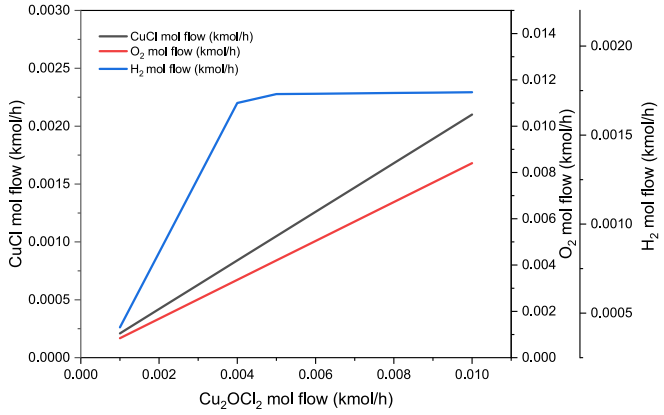



**Fig. 6.** The effect of varying $Cu_2OCl_2$ mole flow rate on the produced CuCl, $O_2$, and $H_2$ mole flow.

but also on whether the reaction is endothermic or exothermic, the reaction enthalpies, and the thermal equilibrium. Therefore, it may not show a proportional increase or decrease for each reaction step. The heat duty of different components in the Cu-Cl system is compared in Fig. 8.

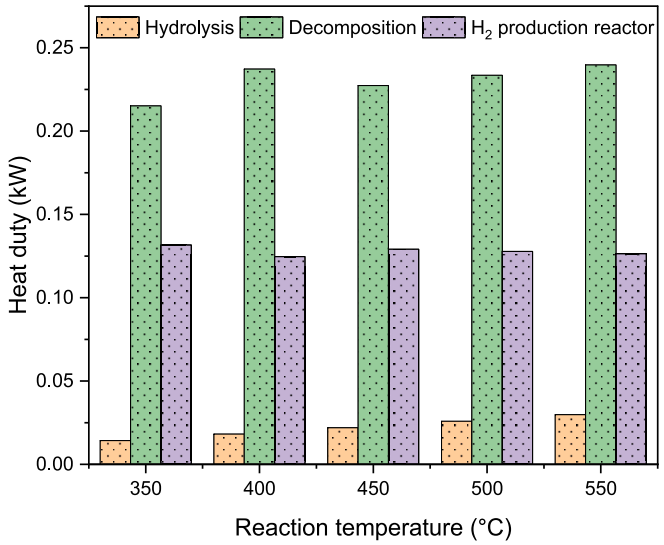



**Fig. 7.** The effect of different reaction temperatures on the heat duty of reactors.

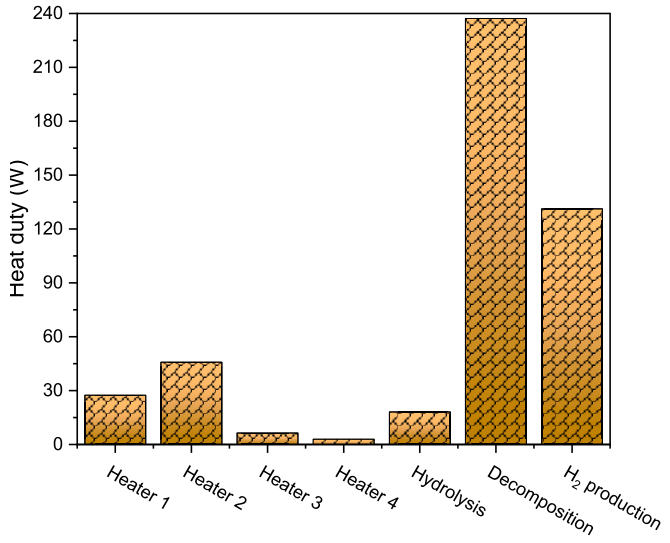



**Fig. 8.** The heat duty capacity of each component in the system.

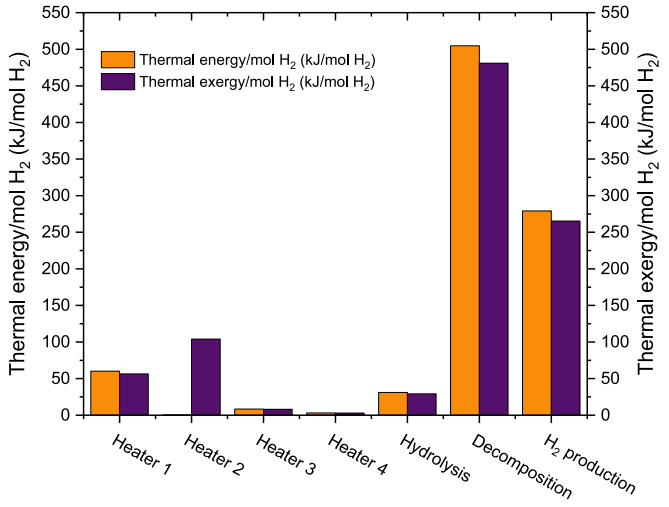



**Fig. 9.** The comparison of thermal energy and thermal exergy values per mole of hydrogen production for each component in the system.

Heater 1 and heater 2 are set to 400 °C and 1 bar to heat the $CuCl_2$ and $H_2O$ reactants to the temperature where the hydrolysis reaction will take place. The temperature and pressure values of the hydrolysis reactor are 400 °C and 1 bar, respectively. Heater 3 and decomposition reaction temperature and pressure are entered as 530 °C and 1 bar as input data. For heater 4 and hydrogen production reactor, input data are 500 °C and 1 bar. Scope of this study, the energy requirements of the components are investigated in the system. It is clearly seen from the graph that the decomposition step has the highest value in terms of heat duty. The decomposition reactor demands a heat duty of approximately 240 W, which shows that the system has the highest energy demand in this step. This situation indicates that the decomposition reaction is a process that requires high energy. The $H_2$ production reactor has the second highest heat load value and stands out as one of the energy-intensive components of the system with a heat load requirement of approximately 120 W. Among the other components, heater 2 and hydrolysis also consume low but significant amounts of energy. However, it is seen that the heat loads of Heater 1, Heater 3, and Heater 4 are quite low. This graph is important in terms of showing the energy distribution in the system and the stages where the highest energy demand occurs. The decomposition and $H_2$ production stages stand out as the most critical processes in terms of energy consumption, and minimizing the thermal load in these stages is of great importance in terms of increasing the overall energy efficiency of the system. It is crucial to compare thermal energy and thermal exergy values per hydrogen of each component in the Cu-Cl thermochemical cycle to determine the energy requirements of the system.

Fig. 9 compares thermal energy and thermal exergy values per mole of hydrogen production for each component in the system, namely Heater 1, Heater 2, Heater 3, Heater 4, hydrolysis, breakdown, and $H_2$ production. The analysis indicated that the decomposition step demonstrated the greatest values of thermal energy and exergy per unit mol of hydrogen. These findings indicate that the process of decomposition is a process that consumes a significant amount of energy, and the system experiences its greatest exergy loss at this step. The hydrogen production step has the second highest thermal energy and exergy value, but the energy and exergy values in this step are lower than the decomposition step. In comparison to the other components, Heater 2 and hydrolysis exhibit somewhat moderate energy consumption, whilst Heater 1, Heater 3, and Heater 4 show rather low energy and exergy values.

In the study conducted by Farsi et al. (Farsi et al., 2019) on the hybrid Cu-Cl cycle, they analyzed the thermal energy supplied and exergy rate required to produce one mole of hydrogen. As a result of their analysis, they calculated the total heat energy required as 2500 kJ/mol $H_2$ and the thermal exergy as 2585 kJ/mol $H_2$. In this study, electrolysis was used in the hydrogen production step and the unit energy consumption of the electrolyzer was determined as 2234 kJ/kmol anolyte. However, in the three-step Cu-Cl cycle proposed in this study, the total thermal energy input was 1660 kJ/mol $H_2$ and the total thermal exergy ratio was calculated as 1625 kJ/mol $H_2$. These values show that the proposed system can provide certain advantages compared to the hybrid systems in the literature in terms of energy and exergy consumption. On the other hand, replacing the electrolysis step with a reactor operating entirely with thermal energy in the proposed cycle eliminates electricity consumption and increases the system's operational simplicity and applicability. In this context, micro-scale experimental studies were also carried out to evaluate the experimental validity of the proposed system. In these experiments, parameters such as $CuCl_2$ and $H_2O$ amounts that directly affect hydrogen production, temperature, time and $CuCl_2$-$H_2O$ ratio affecting the hydrolysis reaction were examined in detail. As a result of parametric studies and optimization studies it was observed that the conditions with the highest hydrogen production were steam/$CuCl_2$ ratio 55, reaction temperature 400 °C, and rection time between 30-40 minutes. Also, it is observed that hydrogen concentration was 134.8 ppm under optimum conditions. Thermodynamic analyses of the proposed three-step Cu-Cl cycle were evaluated using Aspen Plus simulations. Aspen Plus obtains the thermophysical data used in the simulations from extensive databases. These databases include NIST (National Institute of Standards and Technology), DIPPR (Design Institute for Physical Properties), and special thermodynamic models of Aspen Plus. However, there is no direct data in the Aspen Plus library for $Cu_2OCl_2$, one of the components in the system formed after the hydrolysis reaction. Since $Cu_2OCl_2$ is a compound that is not commercially available and is produced at the end of the hydrolysis reaction, Aspen Plus does not include thermophysical data for this compound. To eliminate this deficiency, the molecular weight of $Cu_2OCl_2$ (214 g/mol), enthalpy of formation (−381,300 kJ/kmol) and Gibbs free energy of formation (310,450 kJ/kmol) (Zamfirescu et al., 2010) were added to the Aspen Plus library manually. These values were taken from literature sources and used in the system simulation.

The steam/$CuCl_2$ ratio is a significant parameter that affects the product conversion in the Cu-Cl cycle and directly affects the product efficiency. The effect of the steam/$CuCl_2$ ratio on the production of $Cu_2OCl_2$ and $H_2$ was examined by sensitivity analysis and is given in Fig. 10.

The steam/$CuCl_2$ ratio in the graph is an important parameter in

terms of the reaction kinetics and product efficiency in the Cu-Cl cycle. Steam plays a critical role in hydrogen generation in this cycle. An increase in the $H_2$ mole flow and $Cu_2OCl_2$ mole flow was observed with the increase in the steam/$CuCl_2$ ratio. The reason for this is related to the fact that more steam increases the conversion rate and allows the reactions to proceed more efficiently.

This ratio directly affects the hydrogen production efficiency in particular; because water is one of the main components entering the reaction and is a necessary reactant for the conversion of $CuCl_2$. The primary source of hydrogen in the system is the hydrogen atoms present in water. Higher steam ratios increase the hydrogen yield and allow the reactions to proceed more efficiently. The steam/$CuCl_2$ ratio is seen to be almost constant after 0.52 in terms of the effect on hydrogen production. A high steam ratio can cause $CuCl_2$ to become the limiting reactant by becoming stoichiometrically disproportionate with $CuCl_2$ in the reaction. Furthermore, while the system benefits from steam addition up to a certain point, adding too much steam can negatively affect the reaction kinetics and $H_2$ production can remain constant or decrease. The sensitivity analyses were performed to examine the effect of the conversion ratio on hydrogen production. Fig. 11 shows the amount of hydrogen production with the increase of the conversion rate. It has been observed that as the conversion rate increases, the $H_2$ mole flow (kmol/h) also increases significantly. The conversion rate indicates how much of a chemical reaction is completed, so a high rate indicates that most of the reactants in the system are converted into products.

The exergy destruction is a significant factor that impacts the efficiency of the system. In Fig. 12, the exergy destruction of each component in the system is examined and shown as a percentage. The graph illustrates which processes show the highest exergy destruction. It was found that the decomposition process caused the highest exergy destruction with 50.6 %. It means that decomposition reactions are associated with high energy requirements and irreversible energy losses. It is seen that the hydrolysis process is in second place with 24.7 %. These findings indicate that the decomposition and hydrolysis processes have a major effect on the system's exergy destruction, and that enhancements to these processes can enhance the system's overall efficiency. The ambient temperature is another important factor that affects the system's efficiency.

Fig. 13 shows the effect of ambient temperature ($T_o$) on total energy and exergy efficiencies. While energy efficiency remains constant

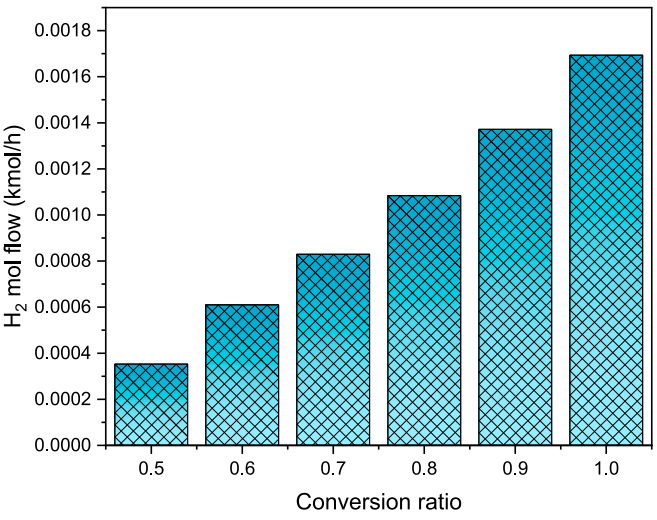



**Fig. 11.** The effect of varying conversion ratio on $H_2$ production rate.

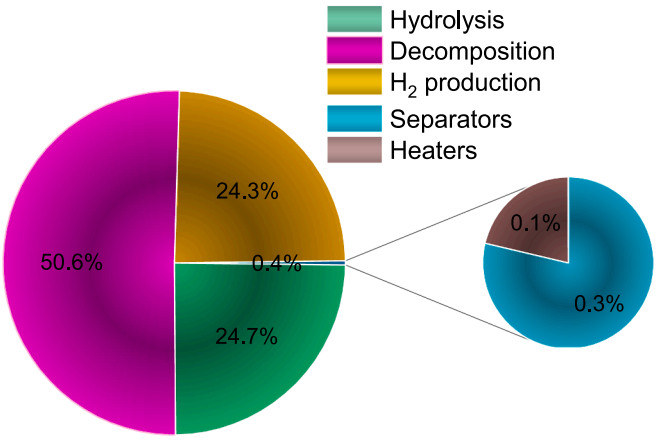



**Fig. 12.** The exergy destruction percentages of each component in the Cu-Cl cyle.

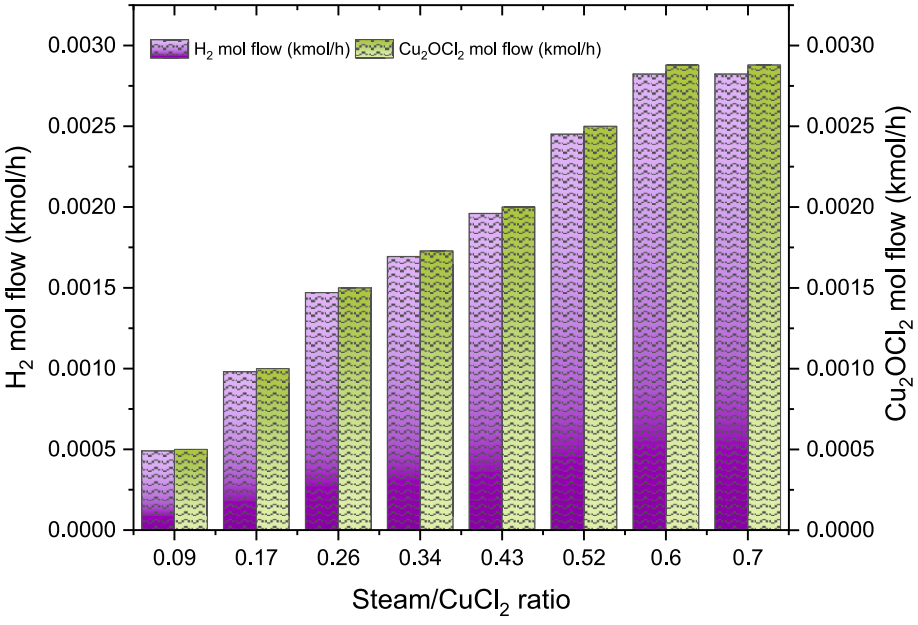



**Fig. 10.** The effect of varying steam/$CuCl_2$ ratio on $H_2$ and $Cu_2OCl_2$ production.

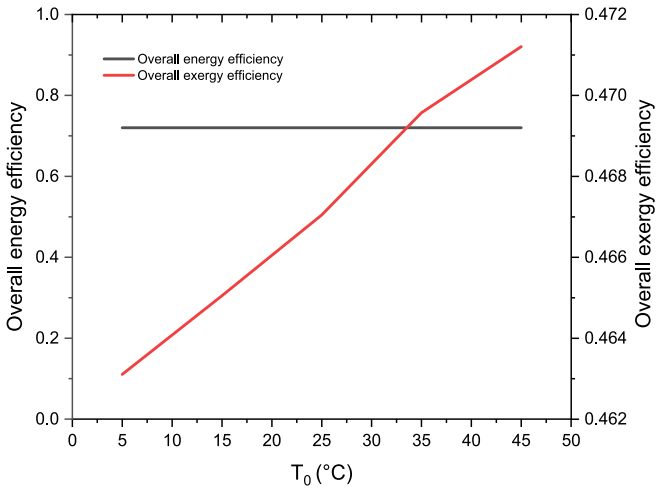



**Fig. 13.** The effect of varying $T_0$ on overall energy and exergy efficiencies of the proposed system.

depending on the ambient temperature change, it has been found that exergy efficiency increases with increasing ambient temperature.

## 6. Conclusions

In the proposed study, a reaction that can replace the electrolysis step in the Cu-Cl thermochemical water splitting cycle, which is one of the clean hydrogen production methods, was theoretically investigated. Thermophysical properties such as temperature, pressure, molar flow rate, molar enthalpy, molar entropy and molar exergy were obtained using the Aspen Plus simulation software, which is important for evaluating the reactor performance and thermodynamic analysis. The sensitivity analyses of the system and a series of parametric studies were performed. According to the sensitivity analyses, it was found that both hydrogen and $Cu_2OCl_2$ production amounts increased with increasing the steam/$CuCl_2$ ratio. These results show that it is critical to carefully optimize the steam/$CuCl_2$ ratio to increase the efficiency in hydrogen and $Cu_2OCl_2$ production. It was observed that the amount of hydrogen production increased in direct proportion to the increasing molar flow rates of $CuCl_2$ and $H_2O$ used in the hydrolysis reaction. As a result of the research on the effect of $Cu_2OCl_2$ mole flow rate on CuCl, $O_2$, and $H_2$ production, it was seen that with increasing $Cu_2OCl_2$ mole flow rate, CuCl and $O_2$ production causes continuous increases, but $H_2$ production reaches a constant value after a certain point. After the impact of different reaction temperatures (350 °C – 550 °C) analysis on the heat duty of three different reactors (hydrolysis, decomposition, and $H_2$ production reactors) in the Cu-Cl cycle, it was found that the decomposition reactor has the highest heat duty of approximately 240 W. Also, it was found that the component with the highest thermal energy required to produce per mol of hydrogen was the decomposition reactor with a value of 504.76 kJ/mol $H_2$. To analyze the system efficiency, exergy destruction analysis of each component in the system was performed. As a result of the analysis, it was found that the component with the largest exergy destruction rate in the system was the decomposition reactor with a rate of 50.6 %. A parametric study was conducted to examine the effect of the ambient temperature on the overall energy and exergy efficiency of the system. As a result of the study, it was observed that the energy efficiency remained constant with increasing temperature, while the overall exergy efficiency increased slightly. Finally, after conducting thermodynamic analyses, overall energy and exergy efficiencies of the system were calculated to be 72.50 % and 46.70 %, respectively.

In the three-step Cu-Cl thermochemical cycle presented, the hydrogen production step includes a hydrogen production reactor operating at high temperatures instead of the electrolysis step. Although this design change supports the increase of energy efficiency, it could decrease the exergy efficiency of the system due to the increased entropy production and thermodynamic losses in reactors operating at high temperatures. In addition, an integration study for thermal management has not yet been carried out in the system. In future studies, it is aimed to increase the exergy efficiency of the presented system by conducting thermal management studies in the system.

## CRediT authorship contribution statement

**Sibel Uygun Batgi:** Writing – original draft, Visualization, Software, Investigation, Data curation, Conceptualization. **Ibrahim Dincer:** Writing – review & editing, Supervision, Resources, Methodology.

## Declaration of competing interest

The authors declare that they have no known competing financial interests or personal relationships that could have appeared to influence the work reported in this paper.

## Data availability

The datasets used in the study will not be available to share.

## References

Abanades, S., Charvin, P., Flamant, G., Neveu, P., 2006. Screening of water-splitting thermochemical cycles potentially attractive for hydrogen production by concentrated solar energy. Energy 31 (14), 2805–2822. https://doi.org/10.1016/j.energy.2005.11.002.

Abdullaev, S., Barakayev, N.R., Abdullaeva, B.S., Turdialiyev, U., 2023. A novel model of a hydrogen production in micro reactor: Conversion reaction of methane with water vapor and catalytic. Internat. J. Thermofluids 20. https://doi.org/10.1016/j.ijft.2023.100510.

Ajeeb, W., Baptista, P., Neto, R.C., 2024. Life cycle analysis of hydrogen production by different alkaline electrolyser technologies sourced with renewable energy. Energy Convers Manag 316. https://doi.org/10.1016/j.enconman.2024.118840.

Al-Zareer, M., Dincer, I., Rosen, M.A., 2018. Transient analysis and evaluation of a novel pressurized multistage ammonia production system for hydrogen storage purposes. J. Clean. Prod. 196, 390–399. https://doi.org/10.1016/j.jclepro.2018.06.022.

Attia, N.F., et al., 2024. Recent advances in sustainable and efficient hydrogen storage nanomaterials. J. Storage Mater. 100, 113519. https://doi.org/10.1016/j.est.2024.113519.

Balashov, V.N., Schatz, R.S., Chalkova, E., Akinfiev, N.N., Fedkin, M.V., Lvov, S.N., 2011. CuCl electrolysis for hydrogen production in the Cu–Cl thermochemical cycle. J Electrochem Soc 158 (3), B266. https://doi.org/10.1149/1.3521253.

Bertino, A., Mazzeo, L., Caputo, G., Sau, S., Giaconia, A., Piemonte, V., 2024. Continuous multiphase Bunsen reactor of iodine-sulfur thermochemical water splitting cycles for hydrogen production: Experimental, Modelling and Design Insights. Chem. Eng. J. 481. https://doi.org/10.1016/j.cej.2023.148415.

Coulibaly, S., Tang, Y., Camara, S., Zhao, J., Li, W., 2022. A theoretical study of molten carbonate fuel cell combined with a solar power plant and Cu–Cl thermochemical cycle based on techno-economic analysis. Int. J. Hydrogen Energy 47 (54), 22680–22690. https://doi.org/10.1016/j.ijhydene.2022.05.030.

Dilmaç, Ö.F., Özkan, S.K., 2008. Energy and exergy analyses of a steam reforming process for hydrogen production. Internat. J. Exergy 5 (2). https://doi.org/10.1504/IJEX.2008.016678.

Dokiya, M., Kotera, Y., 1976. Hybrid cycle with electrolysis using Cu-Cl system. Int. J. Hydrogen Energy 1 (2), 117–121. https://doi.org/10.1016/0360-3199(76)90064-1.

C. Drawer, J. Lange, and M. Kaltschmitt, "Metal hydrides for hydrogen storage – Identification and evaluation of stationary and transportation applications," Journal of Energy Storage, 77, Jan. 30, 2024, doi: 10.1016/j.est.2023.109988.

Farsi, A., Zamfirescu, C., Dincer, I., Naterer, G.F., 2019. Thermodynamic assessment of a lab-scale experimental copper-chlorine cycle for sustainable hydrogen production. Int. J. Hydrogen Energy 44 (33), 17595–17610. https://doi.org/10.1016/j.ijhydene.2019.04.177.

Ferrandon, M., Lewis, M., Tatterson, D., Zdunek, A., 2008. Status of the Development effort for the thermochemical Cu-Cl cycle. In: AIChE Annual Meeting, Conference Proceedings, pp. 1–87. Cincinnati, United States.

Fu, G., He, Y., Zhang, Y., Zhu, Y., Wang, Z., Cen, K., 2016. Catalytic performance and durability of Ni/AC for HI decomposition in sulfur-iodine thermochemical cycle for hydrogen production. Energy Convers Manag 117, 520–527. https://doi.org/10.1016/j.enconman.2016.03.065.

Ghandehariun, S., Naterer, G.F., Dincer, I., Rosen, M.A., 2010. Solar thermochemical plant analysis for hydrogen production with the copper-chlorine cycle. Int. J. Hydrogen Energy 35 (16), 8511–8520. https://doi.org/10.1016/j.ijhydene.2010.05.028.

Ishaq, H., Dincer, I., 2019. A comparative evaluation of three Cu-Cl cycles for hydrogen production. Int. J. Hydrogen Energy 44 (16), 7958–7968. https://doi.org/10.1016/j.ijhydene.2019.01.249.

Kazi, M.K., Eljack, F., El-Halwagi, M.M., Haouari, M., 2021. Green hydrogen for industrial sector decarbonization: Costs and impacts on hydrogen economy in qatar. Comput. Chem. Eng. 145. https://doi.org/10.1016/j.compchemeng.2020.107144.

Lewis, M.A., Ferrandon, M.S., Tatterson, D.F., Mathias, P., 2009. Evaluation of alternative thermochemical cycles - Part III further development of the Cu-Cl cycle. Int. J. Hydrogen Energy 34 (9), 4136–4145. https://doi.org/10.1016/j.ijhydene.2008.09.025.

Lewis, M.A., Masin, J.G., 2009. The evaluation of alternative thermochemical cycles - Part II: The down-selection process. Int. J. Hydrogen Energy 34 (9), 4125–4135. https://doi.org/10.1016/j.ijhydene.2008.07.085.

Li, H., et al., Nov. 2020. Canadian advances in the copper–chlorine thermochemical cycle for clean hydrogen production: A focus on electrolysis. Int. J. Hydrogen Energy 45 (58), 33037–33046. https://doi.org/10.1016/j.ijhydene.2020.09.065.

Y. Li, R. Lin, R. O'Shea, V. Thaore, D. Wall, and J. D. Murphy, "A perspective on three sustainable hydrogen production technologies with a focus on technology readiness level, cost of production and life cycle environmental impacts," 2024, doi: 10.1016/j.heliyon.2024.e26637.

Márquez-Ramos, L., 2018. The environmental impact of renewables. Internat. J. Global Warm. 14 (2), 143–158. https://doi.org/10.1504/IJGW.2018.090176.

Mawdsley, J.R., Carter, J.D., Myers, D.J., Lewis, M.A., Krause, T.R., Aug. 2012. Sulfur trioxide electrolysis studies: Implications for the sulfur-iodine thermochemical cycle for hydrogen production. Int. J. Hydrogen Energy 37 (15), 11004–11011. https://doi.org/10.1016/j.ijhydene.2012.04.133.

Mishra, A., Park, H., El-Mellouhi, F., Suk Han, D., 2024. Seawater electrolysis for hydrogen production: Technological advancements and future perspectives. Fuel 361. https://doi.org/10.1016/j.fuel.2023.130636, 130636.

Montignac, F., Larrahondo Chavez, D., Arpajou, M.C., Ruby, A., 2024. Assessment of hydrogen supply chains based on dynamic bi-objective optimization of costs and greenhouse gases emissions: Case study in the context of Balearic Islands. Energy 308, Nov. https://doi.org/10.1016/j.energy.2024.132590.

Olabi, A.G., et al., 2023. Green hydrogen: Pathways, roadmap, and role in achieving sustainable development goals. Process Safet. Environ. Protect. 177, 664–687. https://doi.org/10.1016/j.psep.2023.06.069.

Ouagued, M., Khellaf, A., Loukarfi, L., 2018. Performance analyses of Cu–Cl hydrogen production integrated solar parabolic trough collector system under Algerian climate. Int. J. Hydrogen Energy 43 (6), 3451–3465. https://doi.org/10.1016/j.ijhydene.2017.11.040.

Ozcan, H., 2015. Experimental and Theoretical Investigations Of Magnesium-Chlorine Cycle and its Integrated Systems. University of Ontario Institute of Technology (Canada).

Ozsari, I., 2023. Trend analysis and evaluation of hydrogen energy and hydrogen storage research. Energy Storage e471, 1–12. https://doi.org/10.1002/est2.471.

Powell, K.M., Edgar, T.F., 2012. Modeling and control of a solar thermal power plant with thermal energy storage. Chem. Eng. Sci. 71, 138–145. https://doi.org/10.1016/j.ces.2011.12.009.

Razmjoo, A., Kaigutha, L.G., Rad, M.V., Marzband, M., Davarpanah, A., Denai, M.J.R.E., 2021. A Technical analysis investigating energy sustainability utilizing reliable renewable energy sources to reduce CO2 emissions in a high potential area. Renewable Energy 164, 46–57. https://doi.org/10.1016/j.renene.2020.09.042.

Roeb, M., et al., 2013. Sulphur based thermochemical cycles: Development and assessment of key components of the process. Internat. J. Hydrogen Energy 6197–6204. https://doi.org/10.1016/j.ijhydene.2013.01.068.

Sattler, C., Roeb, M., Agrafiotis, C., Thomey, D., 2017. Solar hydrogen production via sulphur based thermochemical water-splitting. Sol. Energy 156, 30–47. https://doi.org/10.1016/j.solener.2017.05.060.

Southall, G.D., Khare, A., 2016. The feasibility of distributed hydrogen production from renewable energy sources and the financial contribution from UK motorists on environmental grounds. Sustain Cities Soc 26, 134–149. https://doi.org/10.1016/j.scs.2016.05.009.

Thomas, D., Baveja, N.A., Shenoy, K.T., Joshi, J.B., 2020. Experimental study on the mechanism and kinetics of $CuCl_2$ hydrolysis reaction of the Cu-Cl thermochemical cycle in a fluidized bed reactor. Ind. Eng. Chem. Res. 59 (26), 12028–12037. https://doi.org/10.1021/acs.iecr.0c01807.

Utgikar, V., Ward, B., 2006. Life cycle assessment of ISPRA Mark 9 thermochemical cycle for nuclear hydrogen production. J. Chem. Technol. Biotechnol.: International Research in Process, Environmental & Clean Technology 81 (11), 1753–1759. https://doi.org/10.1002/jctb.1598.

Velasquez-Jaramillo, M., García, J.G., Vasco-Echeverri, O., 2024. Techno economic model to analyze the prospects of hydrogen production in Colombia. Internat. J. Thermofluids 22. https://doi.org/10.1016/j.ijft.2024.100597.

Zamfirescu, C., Dincer, I., Naterer, G.F., 2010. Thermophysical properties of copper compounds in copper-chlorine thermochemical water splitting cycles. Int. J. Hydrogen Energy 35 (10), 4839–4852. https://doi.org/10.1016/j.ijhydene.2009.08.101.

Zhang, B., Shan, S., Zhou, Z., 2022. A novel clean hydrogen production system combining cascading solar spectral radiation and copper-chlorine cycle: Modeling and analysis. J. Clean. Prod. 380. https://doi.org/10.1016/j.jclepro.2022.135036.